Urban Ecosyst (2013) 16:593–616
DOI 10.1007/s11252-013-0291-6

Field and remotely sensed measures of soil and vegetation carbon and nitrogen across an urbanization gradient in the Boston metropolitan area

Preeti Rao · Lucy R. Hutyra · Steve M. Raciti · Adrien C. Finzi

Published online: 23 January 2013

Abstract Understanding the impact of urbanization on terrestrial biogeochemistry is critical for addressing society's grand challenge of global environmental change. We used field observations and remotely sensed data to quantify the effects of urbanization on vegetation and soils across a 100-km urbanization gradient extending from Boston to Harvard Forest and Worcester, MA. At the field-plot scale, the normalized difference vegetation index (NDVI) was positively correlated with aboveground biomass (AGB) and foliar nitrogen (N) content and negatively correlated with impervious surface fraction. Unlike previous studies, we found no significant relationship between NDVI or impervious surface area (ISA) fraction and foliar N concentration. Patterns in foliar N appeared to be driven more strongly by changes in species composition rather than phenotypic plasticity across the urbanization gradient. For forest and non-residential development, soil nitrogen content increased with urban intensity. In contrast, residential land had consistently high soil N content across the gradient of urbanization. When field observations were scaled-up to the Boston Metropolitan Statistical Area (MSA), we found that soil and vegetation N content were negatively correlated with ISA fraction, an indicator of urban intensity. Our results demonstrated the importance of accounting for the influence of impervious surfaces when scaling field data across urban ecosystems. The combination of field data with remote sensing holds promise for disentangling the complex interactions that drive biogeochemical cycling in urbanizing landscapes. Empirical data that accurately characterize variations in urban biogeochemistry are critical to gain a mechanistic understanding of urban ecosystem

Electronic supplementary material The online version of this article (doi:10.1007/s11252-013-0291-6) contains supplementary material, which is available to authorized users.

P. Rao · L. R. Hutyra (✉) · S. M. Raciti
Department of Earth & Environment, Boston University,
685 Commonwealth Ave, Boston, MA 02215, USA
e-mail: lrhutyra@bu.edu

A. C. Finzi
Department of Biology, Boston University, 5 Cummington Street, Boston, MA 02215, USA

function and to guide policy makers and planners in developing ecologically sensitive development strategies.

Keywords Urbanization · Gradient · Vegetation · Soil · Nitrogen · Carbon · Remote sensing · NDVI

Introduction

Urban ecological research is rapidly increasing in importance because of the growing impact of urbanization on the natural environment (Grimm et al. 2008). Urban areas have large ecological footprints (Rees 1992) and their effects on local climate (Zhang et al. 2004a), aquatic ecosystems (Nixon and Fulweiler 2011), the atmosphere (Pataki et al. 2009), energy and material flows (Kennedy et al. 2011) and biogeochemical cycling (Kaye et al. 2006) can reach far beyond their physical boundaries (Grimm et al. 2008; Pickett et al. 2011). It has been estimated that cities are responsible for 71 % of energy-related CO_2 emissions, a figure that is expected to rise to 76 % by 2030 as a result of continued urbanization (Energy Information Administration 2008). Urban areas are also key sources of reactive atmospheric nitrogen and experience enhanced deposition from the by-products of fossil fuel combustion (Lovett et al. 2000; Bettez 2009; Templer and McCann 2010). More than 50 % of the world population lives in urban areas (WUP 2011), where biogeochemical cycles are influenced by complex interactions between biophysical, technical, and socioeconomic systems (Kaye et al. 2006, Kennedy et al. 2011).

Urban ecosystems have received increasing scientific scrutiny in recent years, but many questions about urban biogeochemistry remain unanswered due to complex, often contradictory influences of urbanization on the terrestrial C and N cycles. In regions where closed-canopy forest is the dominant native vegetation, urban development can lead to large decreases in aboveground biomass and net primary productivity (Hutyra et al. 2011a). However, in arid and semi-arid regions, urbanization can have the opposite impact on primary productivity. Kaye and colleagues (2005) found that aboveground net primary productivity (NPP) in the Denver, CO area was four to five times greater in urban land-uses than in natural grasslands. A study by Imhoff and colleagues (2004), which combined satellite data with a terrestrial carbon model, found that urbanization may lead to increased NPP in "resource limited" regions, but decreased NPP in other areas.

Urban areas receive higher rates of atmospheric N deposition (Lovett et al. 2000; Bettez 2009; Templer and McCann 2010) and fertilizer N inputs (Law et al. 2004) than rural areas, but it is unclear to what extent these N inputs lead to systematic changes in canopy N concentrations across urban-to-rural gradients. Evidence from several studies suggests that higher N deposition may result in increased foliar N concentration in hardwood and coniferous forests (Nihlgard 1985; McNulty et al. 1991; Boggs et al. 2005; Fang et al. 2011), however, changes in species composition may complicate our ability to resolve these patterns across urban-to-rural gradients. Plants can also vary in their foliar C:N ratios and their sensitivity to N deposition rates across species and diverse environmental conditions (Aber et al. 2003; Finzi 2009). Furthermore, plants can alter local biogeochemistry, resulting in differences in soil and foliar C and N concentrations and ratios (Finzi et al. 1998; Lovett et al. 2002).

Remote sensing has proven to be a useful tool to detect variations in canopy nitrogen concentrations and hence, map primary productivity at landscape to regional scales (Schimel et al. 1997; Reich et al. 1999; Ollinger and Smith 2005). The instrumentation available for these types of analyses have different tradeoffs in availability, cost of acquisition, revisit

frequency, spectral range, and spatial resolution. Imaging spectroscopy data have been used to estimate canopy chemistry (Wessman et al. 1988; Kokaly and Clark 1999; Curran 2001; Martin et al. 2008) and net primary productivity (Matson et al. 1994; Smith et al. 2002; Ollinger and Smith 2005) in different ecosystems, but are limited by their high cost and restricted flight paths. In contrast, freely available multispectral data from the Moderate Resolution Imaging Spectroradiometer (MODIS) and Landsat satellites are spatially and temporally rich, with global coverage and daily to 16-day return intervals, but have lower spectral resolution. Despite this limited spectral resolution, Landsat-based multispectral vegetation indexes have been shown to significantly capture the variation in foliar nitrogen (Potter et al. 2007; Ollinger et al. 2008) and net primary production (Running et al. 2004; Hollinger et al. 2009) at regional to continental scales.

In addition to aboveground impacts, urbanization also influences soil biogeochemistry. Urban development is associated with physical changes to the landscape, such as increased impervious surface area (Elvidge et al. 2007) and the replacement of natural vegetation with lawns (Milesi et al. 2005), which can positively or negatively alter soil C and N stocks and fluxes (Imhoff et al. 2004; Kaye et al. 2006). Soil studies in Baltimore, MD (Raciti et al. 2011a), Colorado (Kaye et al. 2005; Golubiewski 2006), Oakland, CA (Pouyat et al. 2006), and Chicago, IL (Pouyat et al. 2006) have shown that urban land-uses may have higher soil C stocks than the native ecosystems they replace. Conversely, in regions where native soil pools are richer in carbon, such as Boston, MA (Pouyat et al. 2006; Raciti et al. 2012a) and Syracuse, NY (Pouyat et al. 2006), urban land-uses may have similar or lower soil C stocks. The aforementioned studies examined soils from pervious areas; however, a recent study of the soils beneath impervious surfaces found that C and N losses from these areas may offset sequestration in other parts of the urban landscape (Raciti et al. 2012b), which further complicates these patterns.

While we often conceptualize and categorize areas as urban or rural, there is a continuum in the interactions between the anthropogenic and natural variables across the landscape (McDonnell and Pickett 1990; Stewart 2007). Urbanization gradients can capture this continuum and provide a conceptual framework for understanding anthropogenic effects on basic ecological processes (Pouyat et al. 1995; McDonnell et al. 1997; Idso et al. 2001; Gregg et al. 2003). Quantifying such gradients with measures that capture the variability in urbanization patterns (McIntyre et al. 2000; Luck and Wu 2002; Hahs and McDonnell 2006) could allow for inter-comparison between urban ecological studies. Some of the common metrics used to represent urbanization intensity are distance from urban core (Lovett et al. 2000; Hutyra et al. 2011b; Berland 2012), impervious surface area fraction (Raciti et al. 2012a, Berland 2012), land use (Pouyat et al. 1995; Blair 1996), and landscape fragmentation metrics (Zhang et al. 2004b; Hahs and McDonnell 2006). Inherent differences and complexities arising from variations across biomes, land use history (Foster 1992), and urban development patterns (Seto et al. 2011), suggest that there may not be a single standard set of metrics for quantifying different urbanization gradients (McIntyre et al. 2000). Nonetheless, the challenge in unifying various urban ecological studies rests upon clear characterization of the degree of 'urbanness' and potentially the reporting of a standard set of urbanization metrics (Hahs and McDonnell 2006).

In this study, we used field data from 139 plots to analyze the effects of urbanization on foliar and soil C and N, and vegetation across a 100 km urbanization gradient extending westward from Boston, Massachusetts. In addition, we paired the field measurements with remotely sensed data from Landsat to test our ability to scale up plot-level aboveground variables to the landscape-level (Boston Metropolitan Statistical Area, MSA). We hypothesized that aboveground woody and foliar biomass would decrease with increasing

impervious surface area (ISA), but that foliar and soil N concentrations would be higher in more urbanized areas due to higher local N inputs.

Materials and methods

In this study we used a stratified-random sampling approach and remotely sensed data to quantify the influence of urbanization and land-use on ecosystem characteristics. We collected data on aboveground vegetation biomass, foliar and soil C and N content, and examined relationships between these ecosystem variables, urbanization intensity metrics and Landsat NDVI.

Study area

Approximately 20 % of the US population lives in the large megalopolis extending from Washington, DC to Boston, MA. The Boston MSA, with a population of 4.4 million people, is the 10th most populous metropolitan area in the United States (Census 2010). Our study area extended from coastal Boston, MA westward for 100 km and included transitions from urban to rural areas (Fig. 1). Within this portion of eastern Massachusetts, historical land-use patterns and a complex environmental east-to-west gradient arising from variation in physiography, geology and climate have significantly influenced the vegetation composition and structure (Hall et al. 2002; Foster et al. 2010). By 1850, forest cover in Massachusetts declined to 35 % because of extensive clearing of forested land for agriculture in the late eighteenth century. Subsequently, as the local economy transitioned from agriculture to industry, the forest cover steadily increased to 85 % by 1950. Since then, urbanization, particularly residential and commercial development, has been the major cause for a slow but gradual reduction in forest cover to 63 % (FIA 2005; Foster et al. 2010).

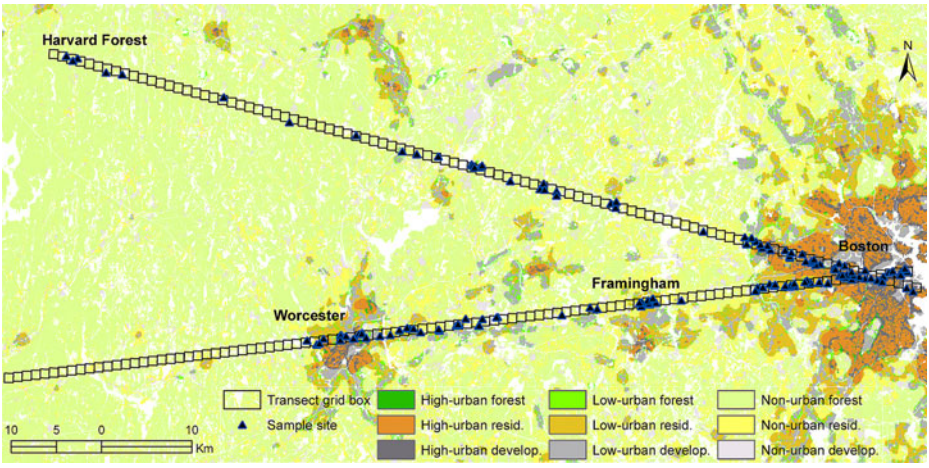

Fig. 1 The map of the study area consisting of 198 adjacent ~1 km^2 grid boxes along the north (98 *grid boxes*) and south (100 *grid boxes*) transects. Approximately 15 plots per sample class (total 139 *plots*) were randomly selected from within these transect grid boxes for field data collection. The nine sample classes based on urbanization intensity and land-use are shown as the map background

The current dominant vegetation type in this region is mixed temperate forests mainly comprising oak (*Quercus spp*.), maple (*Acer spp*.), birch (*Betula spp*.), ash (*Fraxinus spp*.), pine (*Pinus spp*.), and eastern hemlock (*Tsuga Canadensis*; FIA 2005). At the time of European settlement, chestnut (*Castanea dentata*) was also a locally important species, but the chestnut blight has nearly removed its presence from the landscape. The soils are mostly acidic with glacial origins (USDA Natural Resources Conservation Service 2009) and metamorphic bedrock is common, particularly in the Boston MSA (Hall et al. 2002). The Boston region experiences a temperate climate with hot summers (mean daily temperature of 23.3 ° C), cold winters (mean daily temperature of −1.5 ° C) and mean annual precipitation of 105.4 cm$year^{-1}$ spread uniformly across the entire year (National Climatic Data Center 2011).

Field data

The sampling strategy and field data collection protocols for estimating aboveground vegetation biomass and soil chemistry have been described in detail in Raciti et al. (2012a). Here, we summarize these protocols for biomass and soil chemistry and describe the data collection and analysis for foliar chemistry.

Sampling design

We laid out two 100-km transects extending westward from Boston: first, a north transect from Boston to the Harvard Forest long-term ecological research site (Petersham, MA), and second, a south transect from Boston to Worcester, MA (Fig. 1). Linear transects were used to maximize the number of field sample plots while minimizing the amount of travel time between plot locations. This study design also allowed us to compare results from traditional distance-based urbanization metrics (e.g. distance from urban core) with distance-independent measures of urbanization (e.g. impervious surface area fraction in the 1 km^2 neighborhood around each study plot). Both transects originated in downtown Boston (71.04 W, 42.35 N), extended westward on bearings of 284° and 262°, respectively, and then eastward along the same bearings until reaching the coast. The two transects together consisted of 198 adjacent, ~1 km^2 (990 m × 990 m) grid boxes. Stratified random sampling was carried out within these grid boxes by 3 land-use classes and 3 urban classes (9 sample classes in total; Table 1). The three land-use classes were forest, residential, and other-developed (commercial, industrial, and developed open space), based on the 2005 Massachusetts Geographic Information System (MassGIS 2009) land-use/land cover data layer (described in GIS and Remote Sensing Data). We defined an urban intensity class for each ~1 km^2 transect grid box based on two urbanization measures: ISA fraction and population density (see Gradient Characteristics). The three urban classes were high population density urban (ISA>0.25 and population density >2,500 persons km^{-2}), low population density urban (ISA>0.25 and population density <2,500 persons km^{-2}), and non-urban (ISA <0.25) hereafter referred to as high-urban, low-urban, and non-urban (Table 1). For reference, the US Census delineates ‘core’ urban areas using a similar population density threshold of 2,590 persons km^{-2} (1,000 persons mi^{-2}). We identified the threshold for separating urban (ISA≥0.25) from non-urban (ISA<0.25) classes based on the steep drop in ISA when crossing the Interstate-95 corridor around Boston. This threshold defined what we considered to be the urban core of the Boston MSA (Raciti et al. 2012a).

Table 1 The nine sample classes and transect area within each class. These classes were defined based on urbanization intensity and land-use. We obtained land-use information from the Massachusetts land-use/land cover dataset. The three land-use classes were defined by merging different classes from the Massachusetts land-use dataset (see Online Resource 1). Other-developed class consisted of non-residential, developed urban spaces

Urbanization intensity	Land use		
	Forest	Residential (Area in hectares)	Other Develop.
High-urban (High ISA & High Population) ISA>25 %, Population Density >2,500 persons/km^2	49	1,064	1,048
Low-urban (High ISA & Low Population) ISA>25 %, Population density <2,500 persons/km^2	358	938	848
Non-urban (Low ISA & Low Population) ISA<25 %, Population density <2,500 persons/km^2	8,248	2,328	630

We randomly selected 139 sample plots (approximately 15 plots for each of the nine sample classes) and surveyed these for vegetation composition, aboveground biomass, and C and N chemistry of foliage and soil (Raciti et al. 2012a). We obtained prior permissions from property owners of private and governmental land holdings and avoided creating a publically accessible sampling bias by maintaining the public-private land fraction present in the original random draw. All field measurements were made during the 2010 growing season (June-August). In the analysis stage, we reclassified the sample plots based on the ISA and population density of the 1 km^2 area *around each plot* (rather than the original grid-box). Through this process, a few plots were re-categorized into a different sample class.

Data collection

Each sample plot was circular with a 15 m radius (707.14 m^2) and was comparable in size to a Landsat pixel (900 m^2). Within each of the 139 plots, we collected information on plot characteristics such as land-use, canopy cover, tree species composition, and live and dead tree biomass (see Raciti et al. 2012a for a detailed description). We measured the diameter at breast height (DBH; 1.37 m) of all trees with DBH greater than 5 cm and used species-specific allometric equations to estimate total live biomass and foliar biomass (see Data Analysis).

A shotgun is commonly used for collecting foliar samples from different levels of the canopy (Martin et al. 2008). Since a majority of our sample plots belonged to residential and other-developed land-use types, we collected leaf samples using a 5 m tall pole pruner rather than a shotgun. Consequently, foliage was collected from the lower and middle, but mostly sunlit, sections of the canopy for the dominant species present in each plot. We collected five to six leaves from different individuals of the same species, composited them into a single plot sample, dried these samples in the laboratory at 60 ° C for 2–3 days, and stored them for subsequent laboratory analysis.

To determine the soil chemistry, we collected two representative soil samples to a depth of 10 cm from each plot. Soils were sampled to capture the dominant, pervious land covers within each plot. For instance, if the plot consisted of driveway, lawn and a considerable area of bare ground, one soil core was extracted from the lawn and another from the bare ground. Due to logistical constraints associated with sampling on public and private lands, we were

only able to sample and measure soil characteristics within pervious areas, values from Raciti et al (2012b) were used to explore the influence of soils under impervious surfaces. Intact soil cores were brought back to the laboratory and refrigerated at 4 ^{o} C until they could be processed and analyzed for soil moisture, bulk density, and total C and N content (see Laboratory Analysis).

Laboratory analysis

The dried leaf samples were ground and homogenized with a mortar and pestle. We weighed the intact 10 cm deep soil cores, sieved them to remove rocks, coarse roots, and organic material greater than 2 mm in size, and then homogenized the soil samples. Samples were then dried at 60 ° C (until no further change in mass was detectable) and ground into a fine powder with a mortar and pestle. Finally, we loaded subsamples of the homogenized leaf and soil material (2–3 mg and 20 mg, respectively) into 9 × 5 mm tin capsules, placed in sealed microtiter plates, and analyzed for total C and N content by flash-combustion/oxidation using a Thermo Finnigan Flash EA 1112 elemental analyzer (0.06 % C and 0.01 %N detection limits). Samples with known concentrations of C and N were included for every twelve of our samples to confirm the accuracy of the estimates.

GIS and remote sensing data

The following two datasets were downloaded from the MassGIS website: (i) Land-use/land cover vector layer based on 0.5 m digital ortho-images from April 2005 (http://www.mass.gov/mgis/lus2005.htm), and (ii) Impervious surface area (ISA) raster layer with a spatial resolution of 1 m, derived from 2005 near infrared ortho-imagery (http://www.mass.gov/mgis/impervious_surface.htm). We created a population density map using a dasymetric population interpolation method (Langford 2007) whereby we excluded non-habitable areas, such as water bodies and wetlands, and then spatially allocated population to only the residential land cover classes in a census block (Raciti et al. 2012a). The Rogan et al. (2010) Landsat-based vegetation and land cover dataset was used to estimate the proportion of conifer, deciduous and mixed vegetation in the 198 transect grid boxes.

To estimate greenness metrics we downloaded and processed Landsat data covering our transect area (path 12, row 31) for four dates (June 19, July 5, August 14 and 30, 2010), which overlapped with the period of field data collection. We applied atmospheric (Masek et al. 2006) and cloud (Zhu and Woodcock 2012) corrections to the Landsat data and computed the surface reflectance. For each of the 198 transect grid boxes and 139 sampled plots, we computed NDVI, EVI and extracted NIR (0.75–0.90 μm) reflectance values and used their growing season maximum for our analyses. Given that NDVI, EVI, and NIR were found to be highly correlated and NDVI showed the strongest statistical relationships, only the NDVI relationships were reported here. The sample plot, being a circular plot of 30 m diameter, was slightly smaller in area than a 30 m Landsat pixel. To accurately extract the corresponding Landsat reflectance values for the sample plots, we resampled the Landsat data to 3 m and then estimated the average of all the 3 m pixels falling within the plot boundary. Since the 198 transect grid boxes were 1 × 1 km and matched the 1 km spatial resolution of the MODIS products of Gross Primary Productivity (GPP) and Leaf Area Index (LAI), we also downloaded these MODIS products and estimated their 2010 growing season averages for our analysis.

Data analysis

Distance from urban core, ISA fraction, and population density are commonly used metrics of urbanization (McDonnell and Hahs 2008). We compared the suitability of these three metrics for characterizing patterns of development in both the north and south transects of our study area. We found that ISA fraction was the most appropriate metric for urbanization in our study area and used it in our analyses (see Raciti et al. 2012a for a more detailed discussion).

For each sample plot, we estimated aboveground woody and foliar biomass, and soil and foliar C and N content ($g m^{-2}$) and concentration (%). Foliar biomass was estimated using species-specific allometric equations (Tritton and Hornbeck 1982; Ter-Mikaelian and Korzukhin 1997; Jenkins 2004). In the absence of species-specific equations, genus-level or general hardwood (Harris et al. 1973) or conifer (Sollins et al. 1973) equations were applied. Foliar N concentrations for the most abundant tree species (red oak, red maple, sugar maple) were estimated from the mean N concentrations that we measured in leaf samples for those species within a given urban class. Since we had fewer leaf samples from species other than red oak, red maple and sugar maple, we grouped them into hardwood and conifer categories. We calculated foliar N content for each sample plot by multiplying species-specific total foliar biomass and the mean leaf N concentration, again using the hardwood and conifer classes for the less common species. We used the following equation to calculate both soil C and N content (or density at 10 cm depth).

$$W = M_f B_D (1 - \delta_{2mm}) V \quad (1)$$

where W is soil C content, δ_{2mm} is the fraction of material larger than 2 mm diameter, B_D is bulk density, M_f is the fraction by mass of total C, and V is the volume of the soil core (Post et al. 1982). We estimated bulk density of the soil samples by dividing its dry weight by volume ($g cm^{-3}$).

The aboveground and belowground plot-level estimates of C and N content and concentration were scaled to the transect grid boxes by applying the means from the nine sample classes (Table 1) to their respective land areas. The following equation was used to determine all four transect grid (TG) scale estimates of C and N content and concentration for each of the 198 grid boxes.

$$TG = \sum_{i=1}^{9} N_i \times A_i \quad (2)$$

where N_i is the corresponding plot-scale mean value and A_i is the area of each sample class 'i' in the transect grid box. We scaled the soil C and N estimates in two ways. First, we assumed that the soils beneath impervious surfaces were similar in composition to those in the pervious areas of our plots (henceforth referred to as *all-pervious* estimates). Next, we accounted for the altered composition of the soils under impervious surfaces by applying the C and N estimates from Raciti et al. (2012b) to the impervious area of each transect grid box. Raciti et al. (2012b) found that the soils under impervious surfaces in New York City had 66 % and 95 % lower C and N concentrations, respectively, than the soils in nearby pervious areas. We applied those values to the soil under impervious surfaces in each of the 1 km^2 transect grid boxes to arrive at *impervious-adjusted* estimates of soil C and N content and concentration. The purpose of this analysis was to compare the sensitivity of our scaling results to a range of potential assumptions. The *all-pervious* estimates represent an extreme case that will likely overestimate soil C and N stocks, particularly in highly urbanized areas.

We analyzed our field variables at two different scales: plot (~707 m^2) and transect grid (~1 km^2). Using ISA as the urbanization metric, we examined the relationships between the ecosystem variables and urbanization and investigated the relationship of Landsat NDVI with aboveground biomass, foliar N content and concentration. In addition, we also explored whether MODIS GPP and LAI could be used to characterize the urbanization gradient.

Due to the non-normal data distributions, a bootstrapping method was used to determine the 95 % confidence intervals (CI) of different ecosystem variables for the nine sample classes (Efron and Tibshirani 1993). We used non-linear least square to estimate the relationships between different variables, with the non-linear power function having the following form: $y=ax^b$. Goodness of fit on the non-linear curves was assessed with a pseudo-R^2 based on the residual sum of squares for our regressions ($1\text{-}SS_{reg}/SS_{tot}$). The R software package, version 2.12.2, was used for statistical analysis. Unless noted otherwise, all parenthetically reported values are 95 % CI.

Results

Gradient characteristics

ISA and population density varied with distance from the Boston urban core along the two transects with both metrics declining rapidly within the first 20 km from the urban core (Fig. 2a, b). Although these two metrics of urbanization were highly correlated ($R^2=0.76$, $p<0.001$), ISA declined more gradually with distance from the urban core and showed more sensitivity than population density away from the urban core. Hence, we chose ISA as the metric for analysis of the urbanization gradient. For sample plot stratification, we used a combination of ISA and population density to differentiate between the high-urban and low-urban classes (see *Sampling Design*).

The two sample transects captured different urban-to-rural transitions; the north transect quickly transitioned from urban Boston to mostly non-urban areas and small towns and the south transect showed a more varied urban transition, following the Interstate 90 and Route 9 transportation corridors, and passing through secondary urban centers in Framingham and Worcester. The north transect contained 98 grid boxes (Fig. 1), covering a total area of 96 km^2; 21 grid boxes had a mean ISA fraction greater than 0.25. ISA fraction decreased with distance (traveling westward) from downtown Boston with the highest values observed in downtown Boston and the lowest values near the Harvard Forest. The south transect had 100 grid boxes (Fig. 1) covering a total area of 98 km^2. Of these 100 grid boxes, 33 had an ISA fraction greater than 0.25 with the highest values observed in the cities of Boston, Worcester, and Framingham.

The three dominant land-use types across the study area were mixed forest, deciduous forest and low-density residential which together covered nearly 66 % of the total area along each transect. The north transect had more mixed forest (41 % compared to 25 % in S transect; Fig. 2c, d), whereas the south transect had more low-density residential (22 % compared to 8 % in N transect). Both transects had the same proportion of deciduous forest (~17 %; Online resource 1). The other vegetated land-use types (coniferous forest, pasture row crop, orchard and grassland) together covered approximately 10 % of the total area of each transect. The remaining area (~25 %) in each transect was covered by land-use types such as high-density residential, commercial and bare ground.

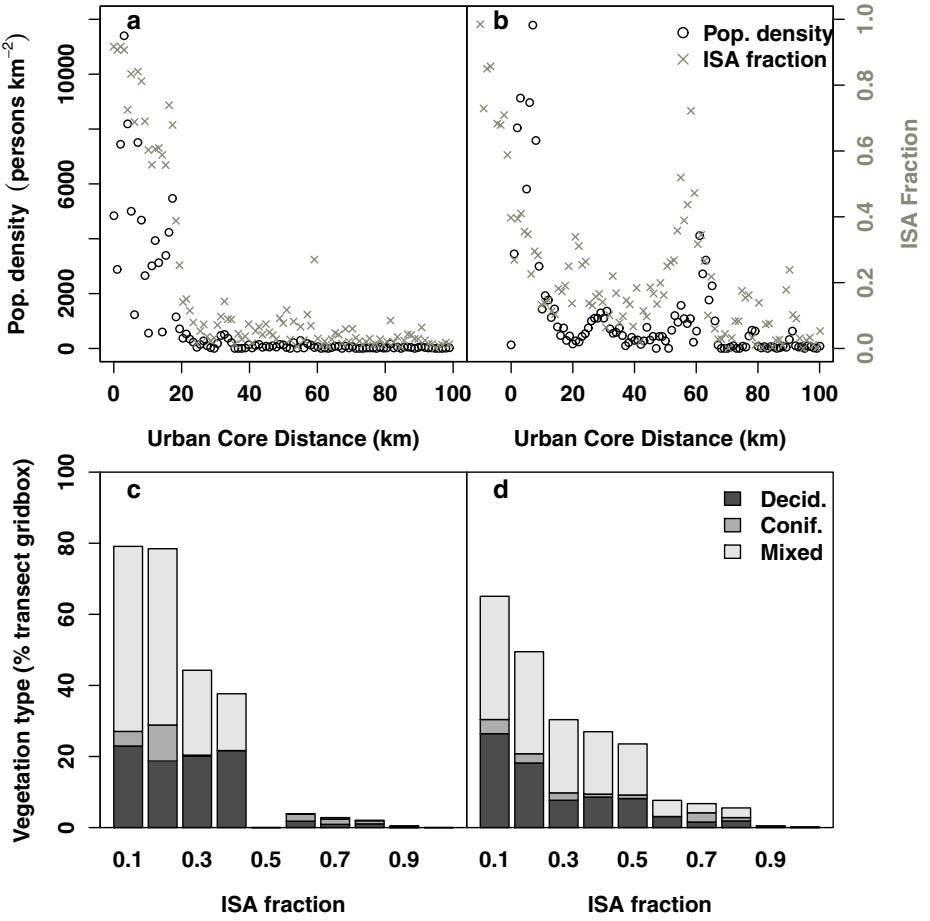

Fig. 2 Urbanization metrics, distance from urban core, impervious surface area (ISA) fraction and population density for the (**a**) north and (**b**) south transects. In the south transect, the peaks at 30 and 60 km from the Boston urban core represent the towns of Framingham and Worcester, MA. The proportions of the three major vegetation types (deciduous, coniferous and mixed) in the transect grid boxes are shown here for the (**c**) north and (**d**) south transects

Aboveground ecosystem variations

Plot-level total aboveground biomass (AGB) was 42 % lower in high-urban (4.0±3.4 kgCm^{-2}) compared to non-urban classes (6.8±3.4 kg C m^{-2}; Table 2) and decreased exponentially from low to high ISA (R^2=0.43, p<0.001, Fig. 3a). Plot foliar biomass decreased consistently from non-urban to urban areas for each of the three sampled land-use classes (forest, residential, and other-developed). Across both transects, the mean foliar biomass of forest (278.6±50.5 g C m^{-2}) was 3.5 times greater than residential (79.4±27.4 g C m^{-2}) and 6 times greater than other-developed (45.5±22.5 g C m^{-2}; Table 2). Differences in foliar biomass amongst the three sampled land-use classes were larger in high-urban areas than in non-urban areas. Foliar biomass in the "forest" class was 16-, 6- and 5-fold higher than that in the "other-developed" class in high-urban, low-urban and non-urban settings, respectively (Table 2).

Table 2 Plot-scale foliar and soil characteristics for the nine sample classes. The number of plots, mean values and 95 % CI for each sample class are given here. Note that biomass and foliar chemistry values were averaged for the entire plot area, while soil values are based on only the pervious portions of the field plots

Plot Variables	High-urban			Low-urban			Non-urban		
	Forest (n=9)	Resid. (n=16)	Oth Dev. (n=15)	Forest (n=19)	Resid. (n=13)	Oth.Dev. (n=19)	Forest (n=16)	Resid. (n=17)	Oth.Dev. (n=15)
Aboveground biomass (kgC m^{-2})	9.46 (7.88)	1.85 (1.67)	0.57 (0.69)	10.57 (2.76)	4.12 (1.62)	1.53 (1.24)	12.36 (2.14)	5.20 (2.33)	2.78 (2.07)
Foliar Biomass (gC m^{-2})	155.47 (78.03)	34.28 (33.62)	10.85 (12.96)	240.62 (56.57)	88.06 (39.02)	42.00 (30.64)	388.39 (83.92)	114.31 (55.51)	79.82 (60.92)
Foliar N content (gN m^{-2})	6.90 (2.46)	2.73 (1.33)	1.76 (0.59)	9.73 (2.57)	3.46 (1.10)	2.75 (0.56)	13.02 (2.76)	6.11 (1.97)	5.84 (2.07)
Foliar %N	2.15 (0.31)	2.08 (0.10)	2.31 (0.05)	2.04 (0.18)	1.81 (0.25)	1.83 (0.17)	1.81 (0.17)	2.10 (0.11)	1.90 (0.14)
Foliar C:N ratio	20.75 (1.88)	23.24 (1.15)	21.40 (0.40)	23.05 (1.57)	28.05 (3.12)	28.82 (2.52)	27.00 (2.49)	23.90 (1.82)	26.38 (1.89)
Soil C content (kgC m^{-2})	4.24 (0.69)	4.45 (0.24)	4.02 (0.37)	3.99 (0.66)	3.72 (0.58)	3.33 (0.58)	4.29 (0.81)	4.02 (0.95)	2.83 (0.47)
Soil N content (gN m^{-2})	236.15 (28.48)	237.39 (9.43)	264.71 (36.53)	214.33 (31.59)	248.76 (32.07)	214.34 (37.90)	203.75 (34.84)	240.44 (23.82)	180.25 (21.28)
Soil %N	0.30 (0.04)	0.28 (0.02)	0.28 (0.04)	0.42 (0.10)	0.29 (0.07)	0.22 (0.04)	0.35 (0.05)	0.34 (0.06)	0.31 (0.10)
Soil C:N ratio	17.95 (3.34)	18.88 (0.92)	16.00 (2.78)	18.48 (2.19)	14.86 (1.17)	15.75 (3.12)	21.90 (1.90)	16.94 (3.11)	16.83 (2.64)

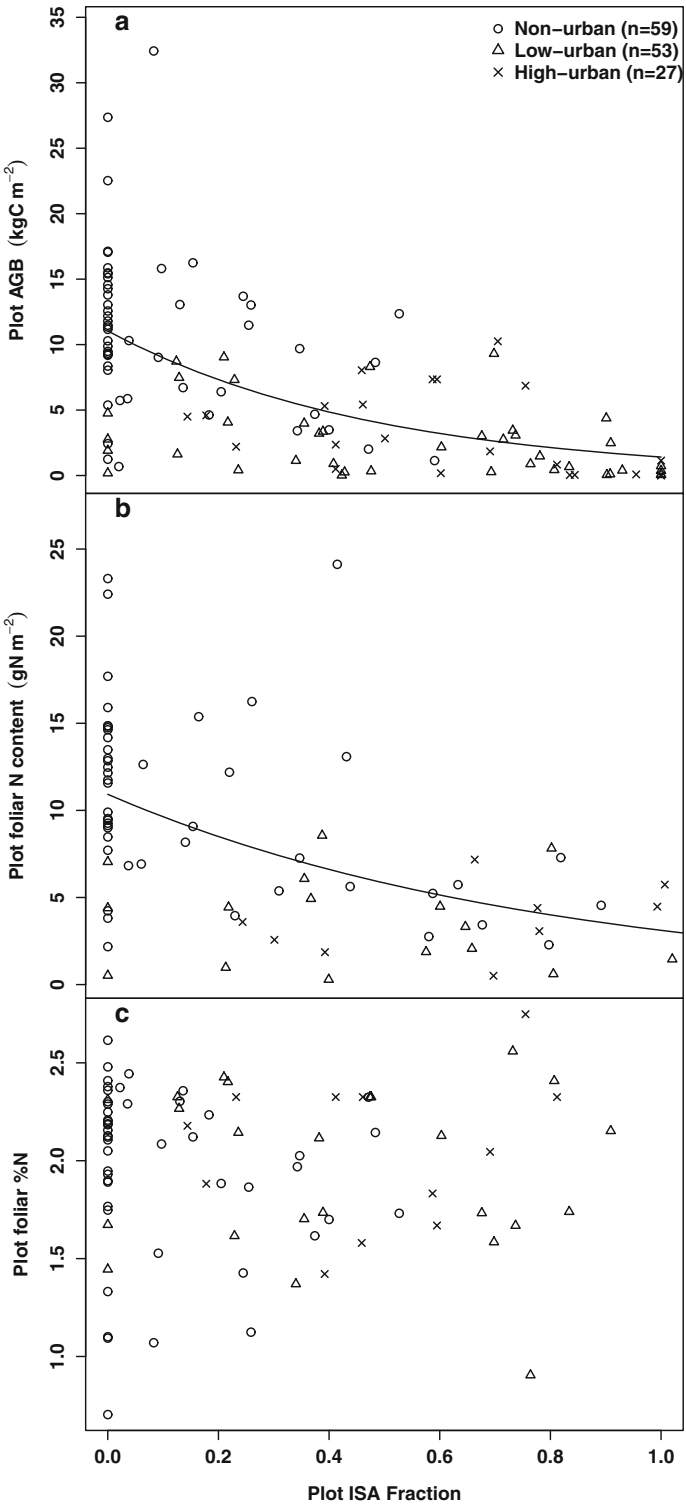
a
Non−urban (n=59)
Low−urban (n=53)
High−urban (n=27)
Plot AGB (kgC m−2)
b
Plot foliar N content (gN m−2)
c
Plot foliar %N
Plot ISA Fraction

◀ **Fig. 3** Relationship between ISA fraction and field measurements of (**a**) plot aboveground biomass (kg C m^{-2}), (**b**) species-weighted average plot foliar N content (g N m^{-2}), and (**c**) species-weighted average plot foliar N concentration (percent). The urban class of each sample plot is based on the urbanization metrics, ISA fraction and population density at 90 m scale

The species-weighted average plot foliar N content, estimated from plot foliar biomass and leaf foliar N concentration, decreased significantly from non-urban to high-urban areas (R^2=0.47, p<0.001; Fig. 3b). This decrease in foliar N content was consistent across each of the three land-use classes. The plot foliar C:N ratio decreased from non-urban forest (27.00±2.49) to high-urban forest (20.75±1.88) and from non-urban other-developed (26.38±1.89) to high-urban other-developed (21.40±0.40). The difference between high- and non-urban residential land-uses was not statistically significant.

Foliar N concentration was significantly higher in red oak (2.36±0.09 %N), sugar maple (2.09±0.14 %N) and other-hardwood (2.32±0.11 %N) than red maple (1.80±0.09 %N) and conifer (1.37±0.17 %N; Table 3). Foliar N concentration of these three species and the two categories (other-hardwood, conifer) showed a tendency for lower values in non-urban than high-urban areas. However, the difference in foliar N concentration due to urban class was statistically significant only for conifers. The three species also showed a higher variability in foliar N concentration in high-urban than non-urban areas (Table 3). The species-weighted average plot foliar N concentration did not show any significant trend with ISA (p=0.57, Fig. 3c) though high-urban plots (2.18±0.15 %N) had higher foliar N concentration than low-urban (1.89±0.20 %N) and non-urban plots (1.94±0.14 %N) (Table 2). Plot foliar N concentration was 19–22 % higher in high-urban forests and other-developed land-use types than in the corresponding non-urban land-use types, but the differences were not statistically significant (Table 2).

Compared to Landsat EVI and the NIR reflectance band, NDVI explained the most variability in aboveground variables, and was highly correlated with measures of vegetation biomass and foliar N content. The mean NDVI for the forest, residential and other-developed land-uses along the gradient was 0.79±0.04, 0.64±0.05 and 0.51±0.06, respectively. For each of these three land-uses, NDVI consistently increased from high- to low- to non-urban. At the plot scale, Landsat NDVI showed negative linear correlation with ISA (R^2=0.66, p<0.001; Fig. 4a) and positive, non-linear correlation with AGB (R^2=0.47, p<0.001; Fig. 4b). NDVI correlated positively and non-linearly with foliar N content (R^2=0.39, p<0.001; Fig. 4c), but there was no significant correlation between NDVI and foliar N concentration (p<0.52; Fig. 4d). In addition to Landsat NDVI, we also examined the relationships between MODIS LAI and GPP with our aboveground field variables. LAI and GPP showed decreasing trends with increasing ISA fraction. However, these trends

Table 3 Mean foliar N concentration with 95 % CI (in parenthesis) of the three major species and two species-categories. We grouped all tree species other than red oak, red maple and sugar maple under other-hardwood and conifer categories

Species or category	Foliar %N (95 % CI)		
	High-urban	Low-urban	Non-urban
Red oak	2.42 (0.13)	2.46 (0.07)	2.26 (0.10)
Red maple	1.74 (0.14)	1.84 (0.10)	1.78 (0.08)
Sugar maple	2.06 (0.24)	2.15 (0.09)	2.01 (0.10)
Other-hardwood	2.46 (0.14)	2.31 (0.10)	2.27 (0.13)
Conifer	1.58 (0.13)	1.37 (0.08)	1.30 (0.13)

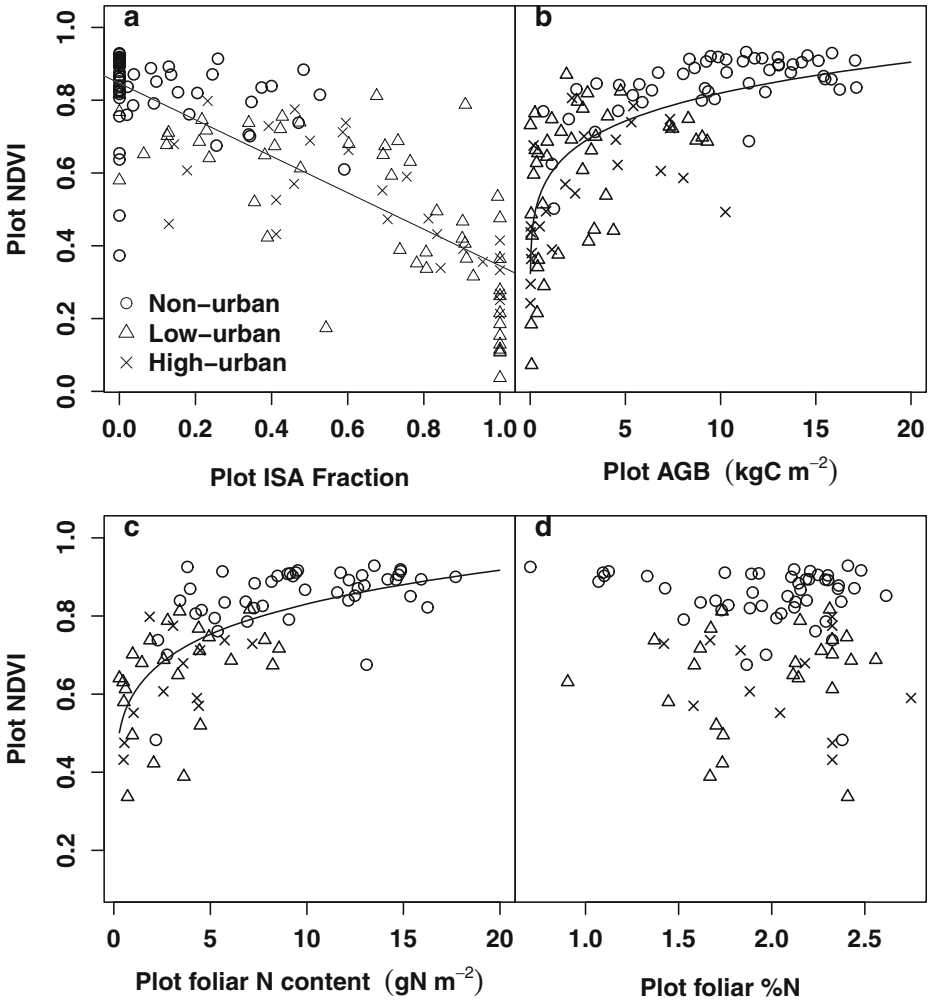

Fig. 4 Plot-scale relationships between growing season mean Landsat NDVI and (**a**) ISA fraction, (**b**) Aboveground biomass (kg C m^{-2}), (**c**) foliar N content, and (**d**) foliar N concentration. The curves in (**b**) and (**c**) show nonlinear least square fit of power function to the data

could not be analyzed across the entire gradient since urban areas (ISA fraction greater than 0.25) are masked out of most MODIS products.

Soil chemistry

Plot-level soil chemistry was measured in pervious areas only (i.e. lawn, garden, bare soil, and forest floor; Table 2). Soil C content increased from non-urban residential (4.02±1.0 to 4.45±0.2 kg C m^{-2}) and other-developed (2.83±0.5 to 4.02±0.4 kg C m^{-2}) classes to their high-urban counterparts and remained consistent across non-urban forest to high-urban forest (4.29±0.8 to 4.24±0.7 kg C m^{-2}; Table 2). Soil N content increased consistently for forest and other-developed classes from non-urban to low-urban to high-urban classes. For residential areas, the soil N content remained high throughout the gradient and did not show

any significant change across the urban classes (Table 2). Soil C:N ratio decreased from non-urban to high-urban forest (21.9±1.9 to 18.0±3.3), while it increased from non-urban to high-urban residential (16.9±3.1 to 18.9±0.9) and remained consistent across the three urban classes of other-developed land-use type. In contrast to the observed trend in soil N content, soil N concentration decreased in the three land-use classes from non-urban to low-urban to high-urban areas, inversely following the measured patterns in soil bulk density (Raciti et al. 2012a). Plot-scale soil C and N content and N concentration did not show any significant trends with increasing ISA fraction.

Ecosystem characteristics at the transect grid scale

Scaling up of the aboveground and belowground plot-level variables to the transect grid scale, weighted by the nine sample classes (Table 1), allowed us to explore neighborhood influences and resulted in some different spatial trends than those observed at the individual plot-level. As the ISA fraction increased, transect scale foliar N content decreased exponentially from 13.1 to 2.1 gNm^{-2} (R^2=0.80, p<0.001; Fig. 5a), showing a trend similar to that of the plot scale (R^2=0.47, p<0.001; Fig. 3b). Foliar N concentration showed a significant positive correlation with the ISA fraction when scaled up to the transect grid scale. It increased from 1.8 to 2.2 % with an increase in ISA (R^2=0.66, p<0.001; *data not shown*) unlike the plot-level results (p=0.57, Fig. 3c).

In the case of soils, *all-pervious* estimates of soil N concentration (0.25 to 0.35 %N) and N content (195.8 to 256.0 gNm^{-2}) were considerably higher than the *impervious-adjusted* estimates at the transect grid scale. However, both these estimates for soil N concentration showed similar trends with an increase in ISA. The *all-pervious* estimates of soil N concentration showed a significant decrease (R^2=0.71, p<0.001) and soil N content showed a significant increase (R^2=0.70, p<0.001) with an increase in ISA fraction, in contrast to the statistically weak trends at plot scale. *Impervious-adjusted* estimates of soil N concentration decreased from 0.35 to 0.01 % with increasing ISA fraction, and was lower in urban areas because of the extremely low values of soil N concentration (0.0057 % for 10 cm depth) under impervious surfaces. Earlier results reported by Raciti et al. (2012a) for soil C and N content did not account for the C and N concentrations under impervious surfaces; and hence showed higher soil C and N content in urban areas. However, estimation of the differences in

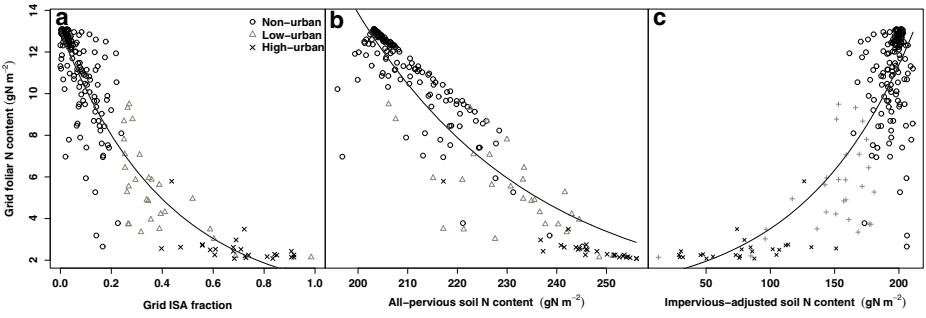

Fig. 5 Transect grid scale relationship between foliar N content and (**a**) ISA fraction, (**b**) *all-pervious* estimates of soil N content, and (**c**) *impervious-adjusted* estimates of soil N content. The urban class of each transect grid box is defined by its ISA fraction and population density. The *all-pervious* estimates are based on the assumption that the soil chemistry beneath impervious surfaces was similar to that in the pervious areas of our plots. The *impervious-adjusted* estimates accounted for the altered composition of soils under impervious surfaces

soil chemistry under impervious surfaces (see Raciti et al. 2012b) resulted in significantly decreasing soil C (4.3 to 1.6 kg C m^{-2}) and N content (211.0 to 12.9 g N m^{-2}) with increasing urbanization; broadly similar to approximations based on clean fill under impervious surfaces (Pouyat et al. 2006; Raciti et al. 2012a).

These differences between *all-pervious* and *impervious-adjusted* estimates of soil N content are further highlighted in their relationship with foliar N content along the gradient. At the transect grid scale, *all-pervious* soil N content had a negative linear correlation with foliar N content (R^2=0.85, p<0.001; Fig. 5b) while *impervious-adjusted* soil N content had a positive exponential correlation with foliar N content (R^2=0.64, p<0.001; Fig. 5c).

Discussion

Urban ecosystem patterns and heterogeneity

Our field observations of aboveground live biomass and C and N content within soils and foliage showed variable relationships with the ISA fraction along our urbanization gradient. Urbanized areas are highly heterogeneous, with large variations in the intensity of land-use, the spatial organization and distribution of different land-uses and covers, species ensembles, land development histories, and underlying abiotic structure. The resultant community of people and flora and fauna across urbanization gradients is the net product of these variations.

The strongest observed relationships between biotic and abiotic data at the plot scale were in aboveground live biomass across the gradient. As the impervious fraction increased and the potential growing space decreased, the observed aboveground live biomass also decreased (Fig. 3a). While this result is intuitive, the field observations also revealed differences between individual land-uses across the gradient (Table 2), with a consistent pattern of decreasing biomass from non- to low- to high-urban. The land cover, as observed and classified through remote sensing, reflects what can be observed from the top-down, but the development intensity and neighborhood context below the vegetation canopy were also strong predictors of the biomass patterns. As reported by Raciti et al. (2012a) the mean aboveground biomass for the Massachusetts portion of the Boston MSA was 7.2±0.4 kg C m^{-2} in 2010, which is substantially greater than the 2.3 kg C m^{-2} reported by Nowak and Crane (2002) for the aboveground live urban carbon density in the City of Boston. This difference in the 'Boston' biomass estimates reflected different definitions of urban and 'Boston' (Raciti et al. 2012a) and the underlying heterogeneity present within different portions of the urban matrix (Table 2). Although variable across the urbanization gradient, the overall aboveground live biomass for high-, low- and non-urban forests (9.5, 10.6 and 12.4 kg C m^{-2}, respectively) was higher than the estimated mean biomass for MA timberlands of 8.5 kg C m^{-2} (FIA 2005). Note that 4.4 million people reside within the Boston MSA (Census 2010) and the mean impervious fraction of this region is 0.17.

Patterns in plot-level foliar N concentrations showed only a weakly positive relationship with ISA across the low- and high-urban classes (Table 2 and Fig. 3c) and there was no significant trend in foliar N concentration in non-urban areas. These weak or non-existent correlations can be attributed, in part, to the variable proportion of hardwood and coniferous species across the study area (Fig. 2c and d). These results are counter to other published studies which reported large differences in foliar N concentration or in N cycling rates between urban, suburban, and non-urban areas (*c.f.* White and McDonnell 1988; Alfani et al. 2000; Zhu and Carreiro 2004; Fang et al. 2011). For example, Fang et al. (2011) reported large differences in foliar N concentration, but also observed very high N deposition (16.2–

38.2 $kgNha^{-1}year^{-1}$) along an urbanization gradient in southern China. Templer and McCann (2010) found lower deposition rates at 14.9±1.7 and 3.6±1.0 $kgNha^{-1}year^{-1}$ in urban and rural sites, respectively, in the Boston area. N cycling rates, which were not directly measured in this study, are another key driver of N concentrations in soil and vegetation and may explain some of the cross-study variability. While soil bulk density (at the plot scale) increased with urbanization across the gradient (Raciti et al. 2012a), soil N content and concentration did not show consistent patterns except for an overall enhancement in residential land-use (Table 2).

When foliar N content was extrapolated to the grid box scale (~1 km^2), we found a negative exponential relationship with ISA (Fig. 5a). This relationship was driven largely by decreases in foliar biomass with ISA, rather than by changes in foliar N concentration across the gradient. We also observed a strong, but negative linear relationship between foliar N concentration and *impervious-adjusted* soil N concentration at the grid box scale ($R^2=0.65$, $p<0.001$; *figure not shown*), which is contrary to studies whose findings did not account for impervious area soils (Nikula et al. 2010; Fang et al. 2011). This result emphasizes the need to account for all cover types, not just pervious areas, when scaling plot-level results to the landscape. The strength of our correlations (Fig. 5a and c) are partly a result of our method of extrapolation, which takes the average soil and foliar N contents from our study transect and applies them to their respective land-uses and urbanization classes.

The overall patterns in foliar N content and concentration across the gradient reflect not only the patterns in ISA and amount of available growing space, but also differences in N deposition and loss, changing floral and faunal compositions, and underlying edaphic factors. Templer and McCann (2010) found 4–5x higher rates of N deposition to a Boston urban forest compared to the rural Harvard Forest, but 10x higher rates of N loss through soil leachate at the urban forest site. In our study we observed changes in the vegetative species composition along the gradient with an increased conifer and mixed vegetation fraction in non-urban areas (Fig. 2c, d); higher foliar N concentrations were observed in hardwood species (Table 3) and in urban land cover classes (Table 2). Additional data such as N deposition and loss, past land use history, species distribution and edaphic conditions would therefore be required to determine the individual and combined influence of these factors on the overall spatial patterns of foliar N content and concentration. As a whole, spatial patterns in vegetation type and the selected scaling methods were found to strongly influence our results and conclusions.

Challenges in urban scaling and comparability

Despite the growing importance of urban areas for global biogeochemistry (Grimm et al. 2008), there is a paucity of data on urban biomass and soil and foliar chemistry. A number of recent review and synthesis papers have highlighted this knowledge gap and summarized the existing observations (Kaye et al. 2006; Pataki et al. 2006; Cadenasso et al. 2007; Pickett et al. 2008; Lorenz and Lal 2009; Pickett et al. 2011), but many of the vegetation and soil biogeochemistry results have been based on markedly different definitions and characterizations of urban (see Raciti et al. 2012a) and have used different sampling and scaling methods. Further, some of the heterogeneity observed in urban areas is likely due to edaphic and land-use history differences rather than urban transformations per se. For example, Lorenz and Lal (2009) compiled a global set of existing organic carbon estimates for urban soils to highlight their heterogeneity, but the underlying biome differences between the study areas have the potential to swamp the urban induced variability.

Two facets of our analysis highlight the sensitivity of cross-site comparisons to differences in urban definition and scaling methodology: the treatment of impervious land areas and the way

that sample class or vegetation type can be used for scaling from field plot to landscape. Estimates of soil C and N content were highly sensitive to whether or not adjustments for soils under impervious surface areas were included (Pouyat et al. 2006; Raciti et al. 2012a; Raciti et al. 2012b). In the case of soils, scaling beyond the plot or pervious surface area typically necessitates adjustments for the commonly unsampled areas below impervious layers since surface soil horizons may be removed during the paving process (Jim 1998) and labile nutrient pools can be lost through time due to continued soil organic matter decomposition in the absence of new organic matter inputs (Scalenghe and Marsan 2009). A recent analysis by Raciti et al. (2012b) found that the concentrations of C and N in soil beneath impervious surfaces in New York City were 66 % and 95 % lower, respectively, than in adjacent pervious-area soils. While the sampling depth intervals differed, these direct measurements of soil chemistry under pavement differed by nearly a factor of two from the 'clean fill' assumptions applied by others (Pouyat et al. 2006; Raciti et al. 2012a). Many analyses of soil C and N content in urban areas have focused on pervious area soils, typically resulting in large increases of soil C and N content with increasing urbanization due to human amendments (Pouyat et al. 2002; Golubiewski 2006; Raciti et al. 2011b). While some studies have tried to account for the influence of impervious surfaces on soil C and N pools, proxies had to be used for the previously unknown composition of these soils (Pouyat et al. 2006, Pouyat et al. 2009, Raciti et al. 2011b). We used the Raciti et al. (2012b) New York City results to adjust for the N composition of impervious covered soils and found that our conclusions were opposite of those that would be drawn from looking at pervious area soils in isolation. Soil N content at the transect grid scale declined steeply (211.0 to 12.9 gNm^{-2}; Fig. 5b) with increasing urbanization. On the other hand, *all-pervious* estimates of soil N content increased (195.8 to 256.0 gNm^{-2}; Fig. 5c) with an increase in urbanization. Our simple *all-pervious* scaling analysis likely over-estimates soil N stocks, but highlights the sensitivity of our results to the range of assumptions that might be used when scaling urban soils data. Our results show that the overall conclusions about regional patterns in soil N content are very sensitive to the inclusion of impervious estimates of soil chemistry and to the exact values that are applied; additional field measurements of soil chemistry below impervious surfaces are needed to better constrain these estimates.

The methods and assumptions used for scaling-up foliar chemistry may also prove important. In this analysis we explored scaling by *sample class* based on land-use and urban classes; however, spatially explicit information on the distribution of tree species or major vegetation types could have provided a more direct physical basis for scaling up foliar C and N content and concentration. Existing remote sensing products in the study area identify broad vegetation classes (hardwood, conifer, mixed forest), but not with great precision. Further, these data are available for many forested areas, but not for the other land-use types that make up much of the study area. The increasing availability of higher resolution remote sensing data and new methods of vegetation spectral analysis hold promise for providing this kind of information in the future. While we were unable to conduct a scaling analysis using detailed, spatially explicit information on vegetation type, the changes in vegetation composition that we observed across the study transects (Fig. 2c and d) and the large differences we measured in foliar chemistry between species and vegetation types (Table 3) suggest that this would be an important factor to consider in future work.

Remote sensing for characterizing urbanization gradients

Remote sensing has been widely applied in urban studies such as mapping land-use and land cover, mapping urban vegetation, and monitoring urban growth and its effects on local climate. Multispectral vegetation indexes have been used successfully to predict foliar

nitrogen and net primary productivity at landscape to regional scales (Potter et al. 2007; Ollinger et al. 2008), but we are unaware of any urban applications. Here, we combined Landsat NDVI with field measurements of foliar N content and concentration and aboveground biomass to explore whether Landsat data could be used to upscale plot measurements along an urbanization gradient. Landsat NDVI correlated well with aboveground biomass (Fig. 4b), foliar biomass (*data not shown*) and foliar N content (Fig. 4c). NDVI is a measure of greenness and is directly related to foliar biomass. Given that foliar biomass exercises a strong control over foliar N content, we observed a significant correlation between NDVI and foliar N content.

To check the robustness of the relationship between NDVI and foliar N content, we calibrated a regression model based on one transect and applied those parameters to predict foliar N content for the other transect. Predicted N content correlated reasonably well with the measured N content along the gradient (R^2=0.40, p<0.01) showing that Landsat data could potentially aid in empirically mapping foliar N content along urbanization gradients. Reliable mapping of foliar N content along urbanization gradients may require integration of other variables. A more direct physical basis for scaling up plot-specific foliar C and N content would be to use spatial data on species composition or major vegetation types, along with plot-specific field estimates of foliar C and N content. Tree species composition, beyond broad conifer/hardwood/mixed classes, has been successfully characterized from remote sensing data in non-urban environments (Martin et al. 1998; Asner et al. 2008), but challenges remain for characterizing vegetation in urban areas. Mixed-pixels (Woodcock and Strahler 1987) make it difficult to differentiate between tree species or even between forest, shrub, and turfgrass vegetation in spatially heterogeneous urban areas (Cadenasso et al. 2007). The move towards higher-resolution remotely sensed data, paired with intelligent object-oriented algorithms, holds promise for better characterizing urban vegetation (O'Neil-Dunne et al. 2012).

In addition to Landsat NDVI, we also examined the relationships between MODIS LAI, GPP and our aboveground field variables. LAI and GPP showed decreasing trends with increasing ISA fraction. However, these trends could not be analyzed for the entire gradient since urban areas are masked out from the standard MODIS products. The spatial resolution of the MODIS LAI and GPP products is 1 km and therefore, too coarse to resolve the vegetative processes in heterogeneous urban landscapes. Milesi et al. (2003) demonstrated that it could be possible to develop 250 m estimates of MODIS LAI and Fractional Photosynthetically Active Radiation (FPAR) by using the 250 m MODIS land cover as an input to the MOD15 Radiative Transfer algorithm, but such a product is currently not available. Fusion of Landsat and MODIS data (Gao et al. 2006) could also provide an opportunity to combine the spatial resolution of Landsat with the temporal resolution of MODIS. Such a dataset might be used to estimate vegetation indexes, FPAR and GPP for characterizing heterogeneous urban landscapes and also, for monitoring temporal changes in productivity.

Conclusions & implications

Urbanization has been shown to have diverse effects on the biogeochemistry of vegetation and soils and is a fundamental driver of current and future global change. Urbanization alters biogeochemical cycling through increased atmospheric N deposition (Templer and McCann 2010), higher temperatures (Zhang et al. 2004a), longer growing seasons (Piao et al. 2008), greater concentrations of ozone (Gregg et al. 2003) and CO_2 (George et al. 2007), altered hydrological flow paths (Kaushal and Belt 2012), and human management activities that

directly alter species composition, disturbance regimes, and water and nutrient availability (Pickett et al. 2011). Urban areas are rapidly expanding, the combination of field data with remote sensing holds promise for helping us detect and understand the complex interactions that drive biogeochemical cycling in urbanizing landscapes. Canopy nitrogen concentration is an important proxy for key ecosystem processes such as N cycling and primary productivity at landscape to regional scales (Schimel et al. 1997; Smith et al. 2002). The ability to remotely sense canopy N concentration across urban to rural gradients could provide new insights about the dynamic interplay between environmental change and ecosystem processes in urbanizing landscapes. In this study we found that NDVI, a remotely sensed index of vegetation, was positively correlated with foliar N content, but not N concentration. Hence, future work might address additional explanatory parameters, such as N deposition, to better predict foliar N at the landscape scale. Impervious surface area fraction, an index of urbanization intensity (Raciti et al. 2012a), was inversely correlated with biomass, foliar N content, and soil C and N contents. For soils, in particular, our results demonstrated the importance of accounting for impervious surfaces (Raciti et al. 2012a and b) when scaling field data across urban ecosystems. Unlike previous studies, we did not find a strong relationship between urbanization and foliar N concentration. Foliar N concentration appeared to be driven more strongly by changes in species composition across the urban-to-rural gradient, rather than the phenotypic changes that might result from increased N inputs. These findings suggest that the influence of urbanization on the environment may be masked or muted by natural variation in soils, vegetation, and climate.

The process of urban development and redevelopment is complex and does not have a predefined trajectory or end point. Inherent edaphic, climatic, and biological variations become intertwined with social, cultural, and economic drivers of development to produce diverse urban environments that evolve over time and space. Within and across urban areas the abiotic growing conditions and biotic compositions can differ markedly from those of natural systems resulting in a unique urban biogeochemistry (Kaye et al. 2006). The dearth of ecological data about urban and urbanizing areas is, in part, a byproduct of the perception that urban ecosystems have limited ecological value because they are heavily modified by humans and are relatively small in size. However, urban areas are rapidly growing in spatial extent and the ecology of cities is becoming more pertinent to people's lives. Empirical data that accurately characterize variations in urban biogeochemistry are critical to gain a mechanistic understanding of urban ecosystem function and to guide policy makers and planners in developing ecologically sensitive development strategies.

Acknowledgements This research was financially supported by the National Science Foundation and US Forest Service Urban Long Term Research Area Exploratory Awards (ULTRA-Ex) program (DEB-0948857), a National Science Foundation CAREER award (DEB-1149471), and Boston University. We are grateful to Marc-Andre Giasson for his help with sample preparation and instrumental analysis; and Max Brondfield and Byungman Yoon for their assistance in field data collection.

References

Aber JD, Goodale CL, Ollinger SV, Smith ML, Magill AH, Martin ME, Hallett RA, Stoddard JL (2003) Is nitrogen deposition altering the nitrogen status of northeastern forests? Bioscience 53(4):375–389

Alfani A, Baldantoni D, Maisto G, Bartoli G, Virzo De Santo A (2000) Temporal and spatial variation in C, N, S and trace element contents in the leaves of Quercus ilex within the urban area of Naples. Environ Pollut 109(1):119–129

Asner GP, Jones MO, Martin RE, Knapp DE, Hughes RF (2008) Remote sensing of native and invasive species in Hawaiian forests. Remote Sens Environ 112(5):1912–1926
Berland A (2012) Long-term urbanization effects on tree canopy cover along an urban-rural gradient. Urban Ecosystems 1–18
Bettez N (2009) Impacts of chronic low level nitrogen deposition along a roadside deposition gradient on forest and estuarine N loading. Ph.D. Dissertation, Cornell University, 93 pp
Blair RB (1996) Land use and avian species diversity along an urban gradient. Ecol Appl 6(2):506–519
Boggs JL, McNulty SG, Gavazzi MJ, Myers JM (2005) Tree growth, foliar chemistry, and nitrogen cycling across a nitrogen deposition gradient in southern Appalachian deciduous forests. Can J For Res-Rev Can Rech For 35(8):1901–1913
Cadenasso ML, Pickett STA, Schwarz K (2007) Spatial heterogeneity in urban ecosystems: Reconceptualizing land cover and a framework for classification. Front Ecol Environ 5(2):80–88
Curran PJ (2001) Imaging spectrometry for ecological applications. International Journal of Applied Earth Observation and Geoinformation 3(4):305–312
Efron B, Tibshirani R (1993) An introduction to the bootstrap. Monographs on Statistics and Applied Probability 57
Energy Information Administration (2008) Emissions of greenhouse gases in the United States. US Department of Energy, Washington, DC
Elvidge CD, Tuttle BT, Sutton PS, Baugh KE, Howard AT, Milesi C, Bhaduri BL, Nemani R (2007) Global distribution and density of constructed impervious surfaces. Sensors 7(9):1962–1979
Fang YT, Yoh M, Koba K, Zhu WX, Takebayashi Y, Xiao YH, Lei CY, Mo JM, Zhang W, Lu XK (2011) Nitrogen deposition and forest nitrogen cycling along an urban-rural transect in southern China. Glob Chang Biol 17(2):872–885
Finzi AC, Van Breemen N, Canham CD (1998) Canopy tree soil interactions within temperate forests: Species effects on soil carbon and nitrogen. Ecol Appl 8(2):440–446
Finzi A (2009) Decades of atmospheric deposition have not resulted in widespread phosphorus limitation or saturation of tree demand for nitrogen in southern New England. Biogeochemistry 92(3):217–229
Forest Inventory and Analysis (2005) http://fia.fs.fed.us/. Accessed 12 October 2011.
Foster DR (1992) Land-use history (1730–1990) and vegetation dynamics in central New England, USA. Journal of Ecology 753–771
Foster DR, Aber JD, Cogbill CV (2010) Wildlands and woodlands: A vision for the New England landscape. Harvard University, Harvard Forest
Gao F, Masek J, Schwaller M, Hall F (2006) On the blending of the Landsat and MODIS surface reflectance: Predicting daily Landsat surface reflectance. Geoscience and Remote Sensing, IEEE Transactions on 44 (8):2207–2218
George K, Ziska LH, Bunce JA, Quebedeaux B (2007) Elevated atmospheric CO2 concentration and temperature across an urban-rural transect. Atmospheric Environment 41(35):7654–7665
Golubiewski NE (2006) Urbanization increases grassland carbon pools: Effects of landscaping in Colorado's front range. Ecol Appl 16(2):555–571
Gregg JW, Jones CG, Dawson TE (2003) Urbanization effects on tree growth in the vicinity of New York City. Nature 424(6945):183–187
Grimm NB, Foster D, Groffman P, Grove JM, Hopkinson CS, Nadelhoffer KJ, Pataki DE, Peters DPC (2008) The changing landscape: Ecosystem responses to urbanization and pollution across climatic and societal gradients. Front Ecol Environ 6(5):264–272
Hahs AK, McDonnell MJ (2006) Selecting independent measures to quantify Melbourne's urban-rural gradient. Landscape and Urban Planning 78(4):435–448
Hall B, Motzkin G, Foster DR, Syfert M, Burk J (2002) Three hundred years of forest and land-use change in Massachusetts, USA. J Biogeogr 29(10–11):1319–1335
Harris W, Goldstein R, Henderson G (1973) Analysis of forest biomass pools, annual primary production and turnover of biomass for a mixed deciduous forest watershed. In: Young H (ed) IUFRO biomass studies, Nancy, France and Vancouver, BC. University of Maine, College of Life Sciences and Agriculture, Orono, ME, pp 41–64
Hollinger DY, Ollinger SV, Richardson AD, Meyers TP, Dail DB, Martin ME, Scott NA, Arkebauer TJ, Baldocchi DD, Clark KL, Curtis PS, Davis KJ, Desai AR, Dragoni D, Goulden ML, Gu L, Katul GG, Pallardy SG, Paw UKT, Schmid HP, Stoy PC, Suyker AE, Verma SB (2009) Albedo estimates for land surface models and support for a new paradigm based on foliage nitrogen concentration. Glob Chang Biol 16(2):696–710
Hutyra LR, Yoon B, Hepinstall-Cymerman J, Alberti M (2011a) Carbon consequences of land cover change and expansion of urban lands: A case study in the Seattle metropolitan region. Landscape and Urban Planning 103(1):83–93

Hutyra LR, Yoon B, Alberti M (2011b) Terrestrial carbon stocks across a gradient of urbanization: a study of the Seattle, WA region. Glob Chang Biol 17(2):783–797
Idso CD, Idso SB, Balling RC (2001) An intensive two-week study of an urban CO2 dome in Phoenix, Arizona, USA. Atmospheric Environment 35:995–1000
Imhoff ML, Bounoua L, DeFries R, Lawrence WT, Stutzer D, Tucker CJ, Ricketts T (2004) The consequences of urban land transformation on net primary productivity in the United States. Remote Sens Environ 89 (4):434–443
Jenkins JC, United States. Forest Service. Northeastern Research S (2004) Comprehensive database of diameter-based biomass regressions for North American tree species. United States Department of Agriculture, Forest Service, Northeastern Research Station
Jim CY (1998) Physical and chemical properties of a Hong Kong roadside soil in relation to urban tree growth. Urban Ecosystems 2(2):171–181
Kaushal S, Belt K (2012) The urban watershed continuum: Evolving spatial and temporal dimensions. Urban Ecosystems 15(2):409–435
Kaye JP, McCulley RL, Burke IC (2005) Carbon fluxes, nitrogen cycling, and soil microbial communities in adjacent urban, native and agricultural ecosystems. Glob Chang Biol 11(4):575–587
Kaye JP, Groffman PM, Grimm NB, Baker LA, Pouyat RV (2006) A distinct urban biogeochemistry? Trends Ecol Evol 21(4):192–199
Kennedy C, Pincetl S, Bunje P (2011) The study of urban metabolism and its applications to urban planning and design. Environ Pollut 159:1965–1973
Kokaly RF, Clark RN (1999) Spectroscopic determination of leaf biochemistry using band-depth analysis of absorption features and stepwise multiple linear regression. Remote Sens Environ 67(3):267–287
Langford M (2007) Rapid facilitation of dasymetric-based population interpolation by means of raster pixel maps. Computers, Environment and Urban Systems 31(1):19–32
Law N, Band L, Grove M (2004) Nitrogen input from residential lawn care practices in suburban watersheds in Baltimore County, MD. J Environ Plan Manag 47(5):737–755
Lorenz K, Lal R (2009) Biogeochemical C and Ncycles in urban soils. Environ Int 35(1):1–8
Lovett GM, Traynor MM, Pouyat RV, Carreiro MM, Zhu W-X, Baxter JW (2000) Atmospheric deposition to Oak forests along an urban-rural gradient. Environ Sci Technol 34(20):4294–4300
Lovett GM, Weathers KC, Arthur MA (2002) Control of nitrogen loss from forested watersheds by soil carbon: Nitrogen ratio and tree species composition. Ecosystems 5(7):712–718
Luck M, Wu J (2002) A gradient analysis of urban landscape pattern: A case study from the phoenix metropolitan region, Arizona, USA. Landsc Ecol 17(4):327–339
Martin ME, Newman SD, Aber JD, Congalton RG (1998) Determining forest species composition using high spectral resolution remote sensing data. Remote Sens Environ 65(3):249–254
Martin ME, Plourde LC, Ollinger SV, Smith ML, McNeil BE (2008) A generalizable method for remote sensing of canopy nitrogen across a wide range of forest ecosystems. Remote Sens Environ 112 (9):3511–3519
Masek JG, Vermote EF, Saleous NE, Wolfe R, Hall FG, Huemmrich KF, Gao F, Kutler J, Lim TK (2006) A Landsat surface reflectance dataset for North America, 1990–2000. Geoscience and Remote Sensing Letters, IEEE 3(1):68–72
Massachusetts Office of Geographic Information, MassGIS (2009) Land Use (2005) data layer. http://www.mass.gov/mgis/lus2005.htm Accessed 2 May 2011.
Matson P, Johnson L, Billow C, Miller J, Pu R (1994) Seasonal patterns and remote spectral estimation of canopy chemistry across the Oregon transect. Ecological Applications 280–298
McDonnell MJ, Pickett STA (1990) Ecosystem structure and function along urban-rural gradients: An unexploited opportunity for ecology. Ecology 71(4):1232–1237
McDonnell MJ, Pickett STA, Groffman P, Bohlen P, Pouyat RV, Zipperer WC, Parmelee RW, Carreiro MM, Medley K (1997) Ecosystem processes along an urban-to-rural gradient. Urban Ecosystems 1(1):21–36
McDonnell M, Hahs A (2008) The use of gradient analysis studies in advancing our understanding of the ecology of urbanizing landscapes: Current status and future directions. Landsc Ecol 23 (10):1143–1155
McIntyre NE, Knowles-Yanez K, Hope D (2000) Urban ecology as an interdisciplinary field: Differences in the use of "urban" between the social and natural sciences. Urban Ecosystems 4(1):5–24
McNulty SG, Aber JD, Boone RD (1991) Spatial changes in forest floor and foliar chemistry of spruce-Fir forests across New-England. Biogeochemistry 14(1):13–29
Milesi C, Elvidge CD, Nemani RR, Running SW (2003) Assessing the impact of urban land development on net primary productivity in the southeastern United States. Remote Sens Environ 86(3):401–410
Milesi C, Running SW, Elvidge CD, Dietz JB, Tuttle BT, Nemani RR (2005) Mapping and modeling the biogeochemical cycling of turf grasses in the United States. Environ Manag 36(3):426–438

National Climatic Data Center (2011) US National Oceanic and Atmospheric Administration (2009) Online Climate Data Directory. http://lwf.ncdc.noaa.gov/oa/climate/climatedata.html.
Nihlgard B (1985) The ammonium hypothesis: an additional explanation to the forest dieback in Europe. Ambio 2–8
Nikula S, Vapaavuori E, Manninen S (2010) Urbanization-related changes in European aspen (Populus tremula L.): Leaf traits and litter decomposition. Environ Pollut 158(6):2132–2142
Nixon SW, Fulweiler RW (2011) Ecological footprints and shadows in an urban estuary, Narragansett Bay, RI (USA). Regional Environmental Change 1–14
Nowak DJ, Crane DE (2002) Carbon storage and sequestration by urban trees in the USA. Environ Pollut 116 (3):381–389
Ollinger SV, Smith ML (2005) Net primary production and canopy nitrogen in a temperate forest landscape: An analysis using imaging spectroscopy, modeling and field data. Ecosystems 8 (7):760–778
Ollinger SV, Richardson AD, Martin ME, Hollinger DY, Frolking SE, Reich PB, Plourde LC, Katul GG, Munger JW, Oren R, Smith ML, Paw UKT, Bolstad PV, Cook BD, Day MC, Martin TA, Monson RK, Schmid HP (2008) Canopy nitrogen, carbon assimilation, and albedo in temperate and boreal forests: Functional relations and potential climate feedbacks. Proc Natl Acad Sci 105(49):19336–19341. doi:10.1073/pnas.0810021105
O'Neil-Dunne JPM, MacFaden SW, Royar AR, Pelletier KC (2012) An object-based system for LiDAR data fusion and feature extraction. Geocarto International 1–16
Pataki DE, Alig RJ, Fung AS, Golubiewski NE, Kennedy CA, McPherson EG, Nowak DJ, Pouyat RV, Lankao PR (2006) Urban ecosystems and the North American carbon cycle. Glob Chang Biol 12 (11):2092–2102
Pataki DE, Emmi PC, Forster CB, Mills JI, Pardyjak ER, Peterson TR, Thompson JD, Dudley-Murphy E (2009) An integrated approach to improving fossil fuel emissions scenarios with urban ecosystem studies. Ecol Complex 6(1):1–14
Piao SL, Ciais P, Friedlingstein P, Peylin P, Reichstein M, Luyssaert S, Margolis H, Fang JY, Barr A, Chen AP, Grelle A, Hollinger DY, Laurila T, Lindroth A, Richardson AD, Vesala T (2008) Net carbon dioxide losses of northern ecosystems in response to autumn warming. Nature 451(7174):49–U43
Pickett STA, Cadenasso ML, Grove JM, Groffman PM, Band LE, Boone CG, Burch WR, Grimmond CSB, Hom J, Jenkins JC, Law NL, Nilon CH, Pouyat RV, Szlavecz K, Warren PS, Wilson MA (2008) Beyond urban legends: An emerging framework of urban ecology, as illustrated by the Baltimore ecosystem study. Bioscience 58(2):139–150
Pickett STA, Cadenasso ML, Grove JM, Boone CG, Groffman PM, Irwin E, Kaushal SS, Marshall V, McGrath BP, Nilon CH (2011) Urban ecological systems: Scientific foundations and a decade of progress. J Environ Manage 92(3):331–362
Population Division of the Department of Economic and Social Affairs of the United Nations Secretariat (2012) World Urbanization Prospects: The 2011 Revision. New York: United Nations
Post WM, Emanuel WR, Zinke PJ, Stangenberger AG (1982) Soil carbon pools and world life zones. Nature 298(5870):156–159
Potter C, Klooster S, Huete A, Genovese V (2007) Terrestrial carbon sinks for the United States predicted from MODIS satellite data and ecosystem modeling. Earth Interactions 11(13):1–21
Pouyat RV, Carreiro MM, Mcdonnell MJ, Pickett STA, Groffman PM, Parmelee RW, Medley KE, Zipperer WC (1995) Carbon and Nitrogen Dynamics in Oak Stands Along an Urban-Rural Gradient. Carbon Forms and Functions in Forest Soils 569–587
Pouyat R, Groffman P, Yesilonis I, Hernandez L (2002) Soil carbon pools and fluxes in urban ecosystems. Environ Pollut 116:S107–S118
Pouyat RV, Yesilonis ID, Nowak DJ (2006) Carbon storage by urban soils in the United States. J Environ Qual 35(4):1566–1575. doi:10.2134/jeq2005.0215
Pouyat RV, Yesilonis ID, Golubiewski NE (2009) A comparison of soil organic carbon stocks between residential turf grass and native soil. Urban Ecosystems 12(1):45–62
Raciti SM, Groffman PM, Jenkins JC, Pouyat RV, Fahey TJ, Pickett STA, Cadenasso ML (2011a) Accumulation of carbon and nitrogen in residential soils with different land-use histories. Ecosystems 14(2):287–297
Raciti SM, Burgin AJ, Man PMG, Lewis DN, Fahey TJ (2011b) Denitrification in suburban lawn soils. J Environ Qual 40(6):1932–1940
Raciti SM, Hutyra LR, Rao P, Finzi AC (2012a) Inconsistent definitions of "urban" result in different conclusions about the size of urban carbon and nitrogen stocks. Ecol Appl 22(3):1015–1035
Raciti SM, Hutyra LR, Finzi AC (2012b) Depleted soil carbon and nitrogen pools beneath impervious surfaces. Environ Pollut 164:248–251

Rees WE (1992) Ecological footprints and appropriated carrying capacity: What urban economics leaves out. Environ Urban 4(2):121–130

Reich PB, Turner DP, Bolstad P (1999) An approach to spatially distributed modeling of net primary production (NPP) at the landscape scale and its application in validation of EOS NPP products. Remote Sens Environ 70(1):69–81

Rogan J, Bumbarger N, Kulakowski D, Christman ZJ, Runfola DM, Blanchard SD (2010) Improving forest type discrimination with mixed lifeform classes using fuzzy classification thresholds informed by field observations. Can J Remote Sens 36(6):699–708

Running SW, Nemani RR, Heinsch FA, Zhao M, Reeves M, Hashimoto H (2004) A continuous satellite-derived measure of global terrestrial primary production. BioScience 54(6):547–560

Scalenghe R, Marsan FA (2009) The anthropogenic sealing of soils in urban areas. Landscape and Urban Planning 90(1–2):1–10

Schimel DS, Emanuel W, Rizzo B, Smith T, Woodward FI, Fisher H, Kittel TGF, McKeown R, Painter T, Rosenbloom N, Ojima DS, Parton WJ, Kicklighter DW, McGuire AD, Melillo JM, Pan Y, Haxeltine A, Prentice C, Sitch S, Hibbard K, Nemani R, Pierce L, Running S, Borchers J, Chaney J, Neilson R, Braswell BH (1997) Continental scale variability in ecosystem processes: Models, data, and the role of disturbance. Ecol Monogr 67(2):251–271

Seto KC, Fragkias M, Guneralp B, Reilly MK (2011) A meta-analysis of global urban land expansion. PLoS One 6(8):e23777

Smith ML, Ollinger SV, Martin ME, Aber JD, Hallett RA, Goodale CL (2002) Direct estimation of aboveground forest productivity through hyperspectral remote sensing of canopy nitrogen. Ecol Appl 12(5):1286–1302

Sollins P, Reichle DE, Olson JS (1973) Organic matter budget and model for a southern Appalachian *Liriodendron* forest. Publ. EDFBIBP-73-2. Oak Ridge National Laboratory, Oak Ridge, TN

Stewart ID (2007) Landscape representation and the urban-rural dichotomy in empirical urban heat island literature, 1950–2006. Acta Climatologica et Chorologica Universitatis Szegediensis, Tomus 40–41

Templer PH, McCann TM (2010) Effects of the hemlock woolly adelgid on nitrogen losses from urban and rural northern forest ecosystems. Ecosystems 13(8):1215–1226

Ter-Mikaelian MT, Korzukhin MD (1997) Biomass equations for sixty-five North American tree species. For Ecol Manag 97(1):1–24

Tritton LM, Hornbeck JW (1982) Northeastern Forest Experiment S Biomass equations for major tree species of the Northeast. US Dept. of Agriculture, Forest Service, Northeastern Forest Experiment Station

U.S. Census Bureau (2010) www.census.gov. Accessed 2 October 2011

USDA Natural Resources Conservation Service (2009). Soil Survey of Middlesex County, Massachusetts.

Wessman CA, Aber JD, Peterson DL, Melillo JM (1988) Remote-sensing of canopy chemistry and nitrogen cycling in temperate forest ecosystems. Nature 335(6186):154–156

White C, McDonnell M (1988) Nitrogen cycling processes and soil characteristics in an urban versus rural forest. Biogeochemistry 5(2):243–262

Woodcock CE, Strahler AH (1987) The factor of scale in remote-sensing. Remote Sens Environ 21 (3):311–332

Zhang XY, Friedl MA, Schaaf CB, Strahler AH, Schneider A (2004a) The footprint of urban climates on vegetation phenology. Geophys Res Lett 31(12)

Zhang L, Wu J, Zhen Y, Shu J (2004b) A GIS-based gradient analysis of urban landscape pattern of Shanghai metropolitan area, China. Landscape and Urban Planning 69(1):1–16

Zhu W-X, Carreiro MM (2004) Temporal and spatial variations in nitrogen transformations in deciduous forest ecosystems along an urban-rural gradient. Soil Biol Biochem 36(2):267–278

Zhu Z, Woodcock CE (2012) Object-based cloud and cloud shadow detection in Landsat imagery. Remote Sens Environ 118:83–94